The University of New Hampshire

Senior Capstone Report

ME 755

Computationally efficient representation of statistically described material microstructure for tractable forming simulations

Author:
Nicholas Landry

Mentor:
Prof. Marko Knezevic

May 16th, 2014

1. Abstract

The purpose of this project is to reduce a large statistical distribution of metal microstructure orientations to a manageable distribution to be used in metal forming simulations. Microstructure sensitive simulations at the macro-scale are impractical, because with so many state variables associated with material microstructure data, these simulations are extremely computationally expensive. [5]

The goal was to develop a framework to accurately model plastic material response while representing the material microstructure in a more compact form, reducing 10^6 or more microstructure orientations to a significantly smaller statistical distribution of representative orientations. This will significantly increase the computational efficiency and make the design process known as microstructure sensitive design (MSD) feasible for industry applications. [1] This framework is applied to metals with both cubic and hexagonal structure to validate this approach for slip and twinning deformation mechanisms.

Performing microstructure sensitive metal-forming simulations is widely recognized as a computational challenge because of the need to store large sets of state variables related to microstructure data. This makes the investigation of the accuracy of smaller, representative data sets in these simulations profitable.

The project accomplished two main goals; the development of an effective fitting algorithm to generate compacted data sets and validation of the framework for data compaction on metals with cubic structure, and hexagonal symmetry, with and without twinning. The research was applied to oxygen-free high-conductivity copper (OFHC Cu) and 6016 aluminum (Al-6016) for application of the framework to cubic metals. An anisotropic (clock-rolled) zirconium (Zr) texture was used to develop the framework for hexagonal metals. The minimum accurate data set for cubic was determined to be 825 orientations and for hexagonal metals, considering twinning and absence of twinning, the minimum number was 1600 orientations. This compaction method will increase the computational speed of microstructure sensitive forming simulations by several orders of magnitude, contributing to the computational feasibility of microstructure informed design.

Contents

List of Figures

2. Introduction and Background

The United States government launched the *Materials Genome Initiative for Global Competitiveness* in June of 2011. This initiative is described as "a unique opportunity for the United States to discover, develop, manufacture, and deploy advanced materials at least twice as fast as possible today, at a fraction of the cost." [4] This project will advance the development and property optimization of metals, which will contribute towards this initiative as a new computational tool.

Currently, the development of new materials is constrained by the microstructure-property linkage. Knowing the microstructure, the material properties can be found, however, this relationship cannot currently be effectively reversed.

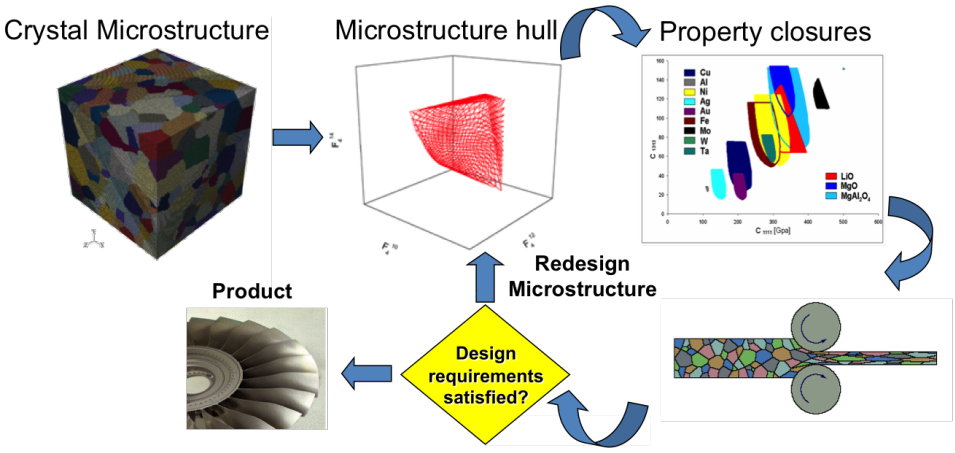

Figure 1. The framework for Microstructure Sensitive Design for Performance Optimization [9]

Historically, no research group has been able to do macro-scale metal-forming simulations informed by the material microstructure because it is too computationally intensive. The resolution of this problem is expedited by with two approaches, first, the development of faster algorithms for solving the stiff and highly non-linear equations governing crystal plasticity, utilizing spectral methods and GPU implementation for up to three order of magnitude increase in computational speedup. Second, speedup can be achieved by reducing the size of the data sets of crystal orientations, which is described in this report. The approach of compact microstructure representation has immediate gains in computational speed and will advent a design process known as "Microstructure Sensitive Design for performance optimization" (MSD) [1] , shown in Figure 1, finding hybrid forming and processing operations to achieve material microstructures necessary to obtain desired material properties.

The framework of this compaction method relies on the expression of the statistical distribution of the material microstructure, known as the orientation distribution function (ODF) [12], as a Fourier series using general spherical harmonics (GSH). The expression of the ODF as a series of Legendre polynomials was developed by H.J. Bunge in 1965 [10]. Theoretically, a material texture can be exactly described as an infinite series of Fourier coefficients, which is the average of the coefficients of each crystal in the polycrystal, which is the statistical collection of all the data points. The

microstructure hull, is the collection of coefficients for each possible material orientation. Though the hull is theoretically in infinite-dimension space, the space can be visualized for the first three Fourier coefficients, shown in Figure 2.

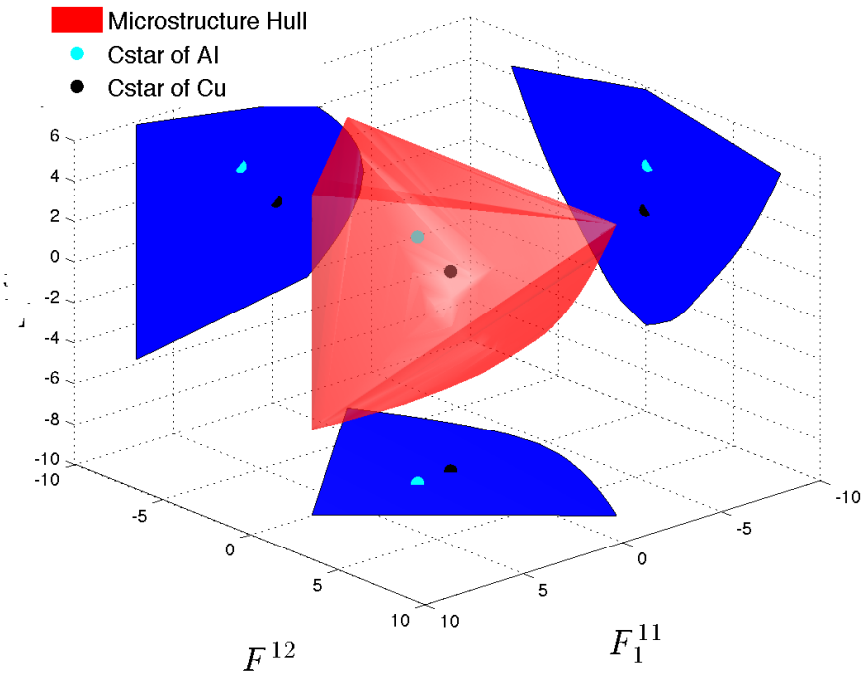

FIGURE 2. The microstructure hull, with two different textures

The importance of this series representation is that the linear structure of the basis can be exploited to construct a linear combination of a compact set of representative orientations to model the experimental microstructure. Crystal plasticity solutions scale linearly between computation time and data set size, so minimizing the data set is a high priority.

3. METHODOLOGY

The methodology for data compaction of the statistical material microstructure data was to transform the crystal orientations of the experimental texture and a smaller, judiciously chosen microstructure data set into the Fourier space as coefficients of a series of Legendre polynomials in general spherical harmonics [10], represented by $T_l^{\mu\nu}(g)$, shown in Figure 3.

3.1. **Framework of Data Compaction.** To transform each orientation into the Fourier basis, the series definition of the ODF, defined as

$$f(g) = \sum_{l=0}^{\infty} \sum_{\mu=1}^{M(l)} \sum_{\nu=1}^{N(l)} F_l^{\mu\nu} \, T_l^{\mu\nu}(g) \tag{1}$$

is used, where $F_l^{\mu\nu}$ is the set of coefficients and $T_l^{\mu\nu}(g)$ is the series of Legendre polynomials. $M(l)$ depends on the crystal symmetry and $N(l)$ depends on the sample symmetry. The base

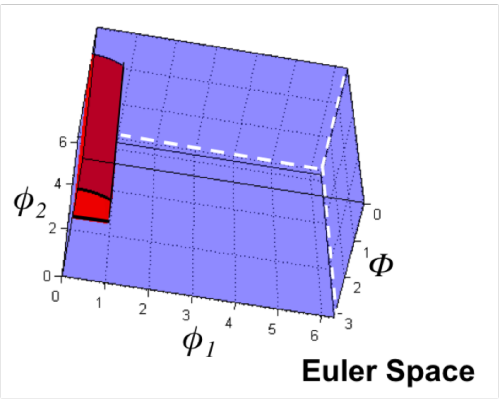

(A) The Euler basis

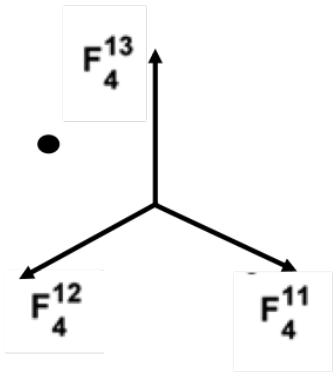

(B) Euler angle transformed into Fourier basis

FIGURE 3. Transformation from the Euler space to the Fourier space [9]

functions $T_l^{\mu\nu}(g)$ are represented in Euler space as the more specific function, $T_l^{\mu\nu}(\varphi_1, \Phi, \varphi_2)$, and are orthogonal functions. [10]

The base functions can be expressed as the following:

$$T_l^{\mu\nu}(\theta, \varphi) = e^{i\mu\varphi_1} P_l^{\mu\nu}(\cos\Phi) e^{i\nu\varphi_2} \tag{2}$$

where $P_l^{\mu\nu}$ is the associated Legendre polynomial [10].

This research is proving the validity of using the series expression of the ODF for data compaction. Three methods of quantification of accuracy of this method are comparing the initial textures, accuracy of the stress-strain response, and comparing the material textures after deformation.

It was proven in previous work [2] that spectral representation of the ODF linearizes the Euler angles that represent the microstructure. This allows the actual material microstructure to be modeled with a significantly smaller set of weighted representative microstructure orientations of equal probability within the Euler Space.

3.2. **Binning of the Euler Space.** The Euler space, a basis representing each physically attainable material orientation, is expressed as $(\varphi_1, \Phi, \varphi_2)$, and can be robustly discretized with the constraint that each bin has equal probability. The equation for the probability (dg) of each bin is [12]

$$dg = \sin(\Phi) d\varphi_1 d\Phi d\phi_2 \tag{3}$$

and the discrete form of this equation is

$$dg = \sin(\Phi) \Delta\varphi_1 \Delta\Phi \Delta\phi_2 \tag{4}$$

where the coarseness of the mesh is determined by the spacing of each angle. The $\sin(\Phi)$ term accounts for the non-linearity of the Euler space when calculating the probability of each bin. The compact, representative ODF to be found in this study is the binning with the minimum number of orientations, is able to match the original material texture with an acceptable level of accuracy.

The binning is different with different crystal symmetries, because the bounds of the Euler space change due to redundancies present in the crystal symmetry. The bounds of the Euler space for orientations with cubic symmetry are

$$\left((\varphi_1,\, \Phi,\, \varphi_2) \middle| \, 0 \leq \varphi_1 < 2\pi,\, \arccos\left(\frac{\cos\varphi_2}{\sqrt{1+\cos^2\varphi_2}} \right) \leq \Phi \leq \frac{\pi}{2},\, 0 \leq \varphi_2 \leq \frac{\pi}{4} \right) \tag{5}$$

where the φ_2 dependency of φ_1 is due to the redundancy of the cubic symmetry [12]. For orientations with hexagonal symmetry, the bounds of the Euler space are

$$\left((\varphi_1,\, \Phi,\, \varphi_2) \middle| \, 0 \leq \varphi_1 < 2\pi,\, 0 \leq \Phi < \frac{\pi}{2},\, 0 \leq \varphi_2 < \frac{\pi}{3} \right) \tag{6}$$

Bounds on the Euler space effectively represent the physically realizable orientations for a given material symmetry, and allow a representation without redundancies to be constructed. The Euler space with the bounds for a particular symmetry, is known as the fundamental zone, or FZ.

Since each point in the discretized Euler space is mapped to the Fourier basis, the most effective binning will be able to match any texture within the microstructure hull shown in Figure 2 for the number of coefficients that provide sufficient accuracy, for the minimum data set size. A binning that transforms to the vertices of the microstructure hull is the most effective.

3.3. **Improving Binning of the Euler Space.** Using the basic theory behind the Nyquist sampling theorem, we changed the discretization of each angle of the Euler space to accurately and robustly represent every point within the microstructure hull to a maximum number of dimensions. We assume that though the Euler angles are dependent rotations, they may be treated independently in Euler space.

Euler Angle	Corresponding Index
φ_1	n (ν)
Φ	l
φ_2	m (μ)

TABLE 1. Correspondence between Euler Space and GSH Functions

For hexagonal symmetry, optimum binning was determined to be to discretize φ_1 4N times, *Phi* 4N times, and φ_2 N times, where $N = 2 \ldots \infty$. For cubic symmetry, only a weak dependence on discretization choice was observed, so the discretization was φ_1 $8(N-1)+1$ times, Φ $(N-1)+1$ times, and φ_2 $(N-1)+1$ times, where $N = 2 \ldots \infty$, because of the fairly even angle discretization. N indicates the fineness of the mesh desired.

Improving the binning resulted in more coefficients being fit with smaller data sets. This significantly impacted the compaction of the data; without changing the discretization, 16393 orientations fit 27 unique, non-zero dimensions, and after improving the discretization, 1600 orientations can fit 101 unique dimensions in the Fourier space. The speed also improved considerably using *linprog*;

the greedy algorithm fit 27 dimensions with 1.8 million iterations, taking about 30 minutes, whereas *linprog* fit 245 dimensions with 50 iterations, taking approximately 45 seconds on a standard CPU.

3.4. **Fitting Algorithm.** When a statistical material texture is described in the Fourier space, it is represented as the average of the Fourier coefficients for each orientations in a polycrystal. Each orientation of a carefully selected representative texture, using the binning scheme described, can also be transformed into the Fourier space. To find the distribution associated with the representative texture, the following constrained linear system needs to be solved. The elegance of the series representation of the statistically described microstructure is that by transforming the ODF into Fourier space, the linear properties of the basis are exploited.

The equations and constraints to find the statistical distribution of orientations for a representative texture in Fourier space are the following:

$$\mathbf{F}_{ij}\vec{\alpha}_i = \vec{C}_j^* \tag{7}$$

$$\alpha_i \geq 0 \tag{8}$$

$$\alpha_i \leq 1 \tag{9}$$

$$\sum_{i=1}^{N_{crys}} \alpha_i = 1 \tag{10}$$

$\mathbf{F}$ is the matrix of coefficients for each representative orientation, of size $(N_{crystals} \times N_{dimensions})$, and where α_i is the volume fraction of each individual orientation. C^* is the vector of average Fourier coefficients of the objective texture to be fitted. α_i is limited in value between 0 and 1 because it is non-physical to have a negative or greater than unity volume fraction.

As the number of coefficients fitted in this framework approaches infinity, the representative texture being fitted will become identical to the target ODF.

3.4.1. *Greedy Algorithm.* The original fitting algorithm was a dynamic programming scheme that obtains a linear combination of these representative orientations matching the actual average vector in Fourier space, using the following equation to optimize the weight of an additional crystal to the existing average at each iteration. The equation is [1]

$$\alpha = \sum_{l,\mu,\nu} \frac{\left(C_l^{*\,\mu\nu} - A_l^{*\,\mu\nu}\right)\left(F_l^{\mu\nu} - A_l^{*\,\mu\nu}\right)}{\left(F_l^{\mu\nu} - A_l^{*\,\mu\nu}\right)^2} \tag{11}$$

and once a new $F_l^{\mu\nu}$ is found that has a linear combination that is closest to C^*, the new average is given by

$$A^{*\,new} = \alpha\left(A_l^{*\,\mu\nu}\right) + (1-\alpha)F_l^{\mu\nu} \tag{12}$$

The limitations of using this algorithm is that when fitting textures close to the surface of the texture hull, this method is quite inefficient.

[1]Where l, μ, and ν are the indices of the specialized functions, C^* is the average experimental Fourier coefficient, A^* is the current average Fourier coefficient, and $F_l^{\mu\,\nu}$

3.4.2. *MATLAB: Linear Programming.* For a more sophisticated solution method, MATLAB's *linprog* function was used. This MATLAB function is based on the interior point method, and the system of equations is modified to accommodate this solver.

The modified system of equations is the following:

Equality Constraints

$$\mathbf{F}_{ij}\vec{\alpha}_i - \vec{C^*}_j - \vec{t_{1,j}} + \vec{t_{2,j}} = 0 \tag{13}$$

$$\sum_{i=1}^{N_{crys}} \alpha_i = 1 \tag{14}$$

Inequality Constraints

$$\text{Lower Bound: } \alpha_i \geq 0 \tag{15}$$

$$t_1, t_2 \geq 0 \tag{16}$$

$$\text{Upper Bound: } \alpha_i \leq 1 \tag{17}$$

Minimize the following equation:

$$\sum_{i=1}^{N_{dim}} (t_{1,i} + t_{2,i}) \tag{18}$$

In this formulation, $\vec{t_1}$ and $\vec{t_2}$ are slack variables. The slack variables are utilized because they allow the linear system to become an equality constraint. These slack variables are bounded so that they cannot stay "hidden" when minimizing their sum. They are always positive, guaranteed by the bounds, however, in the equality constraint, the addition and subtraction means that there is more flexibility when arriving at a solution. In MATLAB, the α_i, and the slack variables are all components in a solution vector g.

To express this in a form for use in MATLAB, the equality equations become the following:

$$\begin{bmatrix} \left(\mathbf{F}^T\right)_{N_{dim}\times N_{crys}} & (\mathbf{I})_{N_{dim}\times N_{dim}} & -(\mathbf{I})_{N_{dim}\times N_{dim}} \\ (1)_{1\times N_{crys}} & (0)_{1\times N_{dim}} & (0)_{1\times N_{dim}} \end{bmatrix} \begin{pmatrix} \vec{\alpha_i} \\ \vec{t_1} \\ \vec{t_2} \end{pmatrix} = \begin{pmatrix} (C^*)_{N_{dim}\times 1} \\ 1 \end{pmatrix} \tag{19}$$

This solution method is only feasible when point to be fitted is within the microstructure hull, because interior point algorithms assume that the solution will be located in a feasible region with the given constraints. If the point lies outside this region, interior point methods heavily penalize the function to be optimized.

This algorithm converges much more rapidly, as shown in Figure 4. The convergence of the primal and dual problems is robust and for this research, we assumed that a robust solution was present when the distance between the primal and dual was less than 1×10^{-8}.

To improve the smoothness of the ODF, when possible, we constrained the maximum volume fraction of a crystal orientation to be less than $\frac{10}{N_{crystals}}$, to prevent any tendency of the ODF to a single crystal.

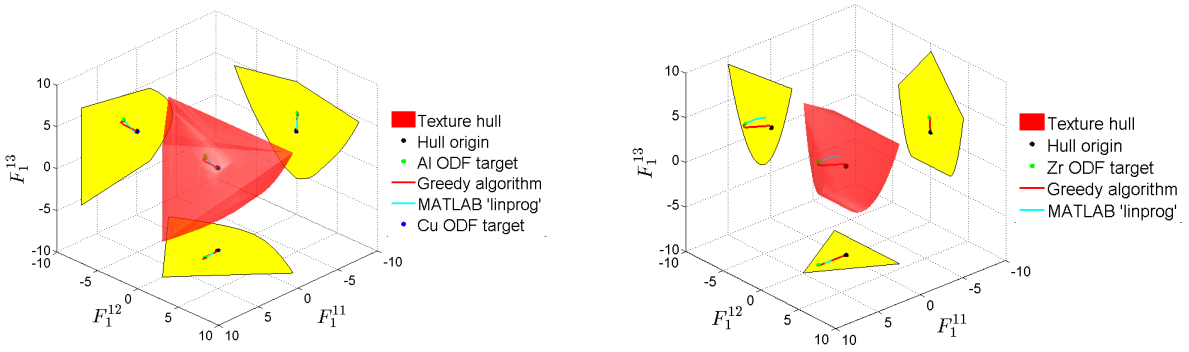

(A) Hull with cubic symmetry, fitted to l=12 (B) Hull with hexagonal symmetry, fitted to l=6

FIGURE 4. Fitting within the texture hull, for cubic and hexagonal metals, using two different algorithms.

The improved fitting also improves the accuracy of the representative ODF, shown in Figure 5.

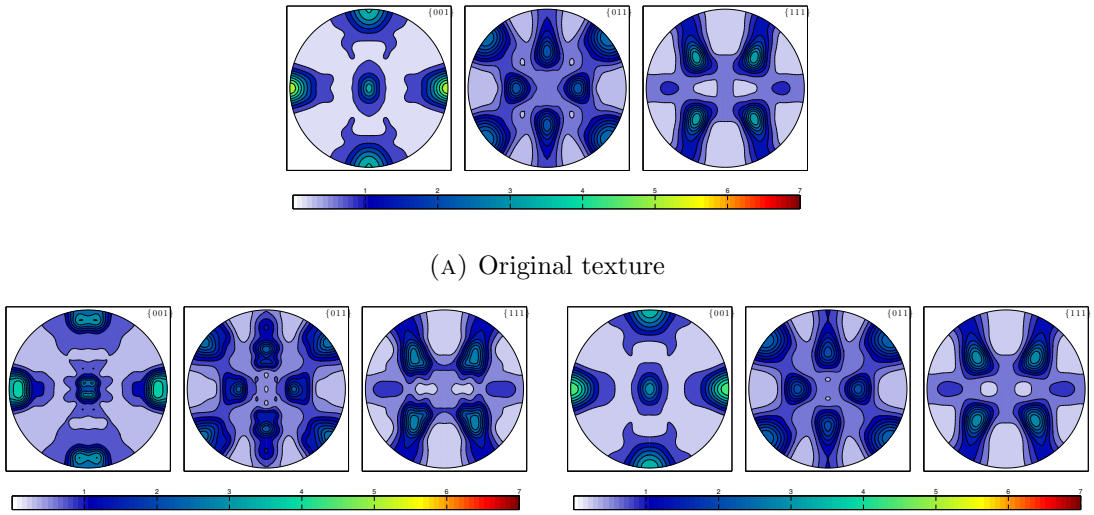

(A) Original texture

(B) Greedy algorithm (C) linprog

FIGURE 5. Pole figures for Aluminum, using the greedy algorithm and MATLAB's *linprog*

3.5. **Pole Figures.** Pole figures are a visual representation of the statistical distribution of material orientations [12]. If two textures both have the same pole figure representation, they will be identical textures. In this research, the MTEX package for MATLAB was used to generate the pole figures, because of its advanced smoothing options. The Bunge-Euler angle convention was used when describing the statistical material microstructure.

3.6. **Stress-Strain Response.** The stress-strain response was generated at a single integration point of the material, assuming a statistical polycrystal. The Visco-Plastic Self-Consistent (VPSC) code, version 7c, was used when calculating the plastic material response. This code was developed

by C.N. Tomé and R.A. Lebensohn at Los Alamos National Laboratory to generate microstructure sensitive stress-strain response and texture evolution using crystal plasticity constitutive laws. It accounts for slip and twinning deformation mechanisms, and hardening, reorientation and shape change of individual grains [11].

The goal of this project was not to improve the accuracy of microstructure sensitive simulations, but to prove that a compact representative microstructure behaves very similarly to a much larger original data set. Therefore, our goal is consistency, not accuracy, because the conclusions of this research will provide a useful tool for improving the modeling of these simulations.

3.7. **Texture Difference.** For the use of this research, we created a mathematical tool for defining the differences in texture called the texture difference index (TDI). It is defined in the Fourier space as the distance between the original microstructure's average Fourier coefficients, known as C^*, and the representative texture's average Fourier coefficients, all normalized by the maximum distance from the original microstructure's texture within the texture hull. The equation is given as

$$TDI = \frac{\sqrt{\int\limits_{FZ} \left(f^*(g) - \bar{f}(g)\right)^2 dg}}{\sqrt{\int\limits_{FZ} \left(f^*(g) - \tilde{f}(g)\right)^2 dg}} = \frac{\sqrt{\sum\limits_{l,\mu,\nu} \left(F_l^{*\mu\nu} - \bar{F}_l^{\mu\nu}\right)^2}}{\sqrt{\sum\limits_{l,\mu,\nu} \left(F_l^{*\mu\nu} - \tilde{F}_l^{\mu\nu}\right)^2}} \tag{20}$$

where the $F_l^{*\mu\nu}$ coefficients correspond to the original texture, the $\bar{F}_l^{\mu\nu}$ coefficients correspond to the compact, representative texture, and the $\tilde{F}_l^{\mu\nu}$ coefficients correspond to a single crystal that is farthest away from the target texture. [2]

Using this definition, an identical texture has a TDI of 0, and the texture with the greatest misorientation has a TDI of 1. The number of dimensions to which this texture difference is computed is the maximum number of dimensions to which a representative texture has been computed. For cubic metals, we chose $l = 16$ and for hexagonal metals, we chose $l = 20$.

4. Results

Implementing the theory described in the section on methodology, we validated this data compaction framework with three methods described in the previous section. First, the initial representative ODFs are compared with the experimental ODFs to evaluate the effectiveness of generating an initial texture using the GSH series approach to ODF representation. Secondly, the generated textures were used in simulations of different loading conditions, to evaluate whether the smaller, representative texture could accurately model the response of the polycrystal, with different deformation mechanisms, such as crystal slip and twinning. Lastly, the difference in texture was measure after deformation to examine whether the smaller data set was able to capture the texture evolution occurring due to crystal plasticity.

[2] In this formulation, $\int\limits_{FZ} f^*(g)dg = \int\limits_{FZ} \tilde{f}(g)dg = \int\limits_{FZ} \bar{f}(g)dg = 1$ which represents the probability, or volume fraction [12]

4.1. **Initial Texture Comparisons.** The initial textures fitted had cubic and hexagonal symmetries, to broaden the impacts of this research for application to a diverse set of materials. The pole figures were compared to see if the representative textures captured the statistical distribution of material orientations.

For cubic metals, the initial pole figures are shown in Figure 6.

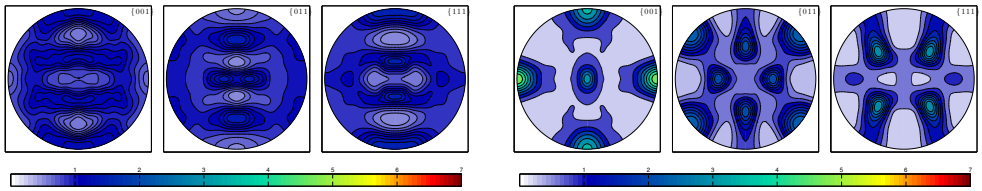

(A) Original Texture

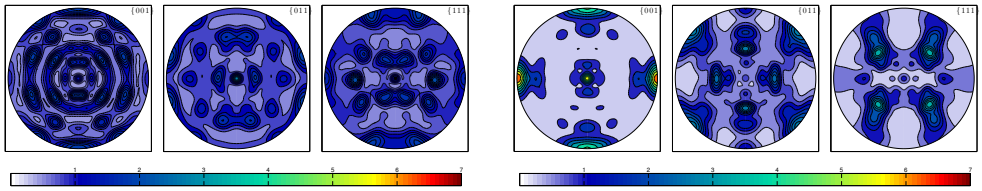

(B) 153 orientations

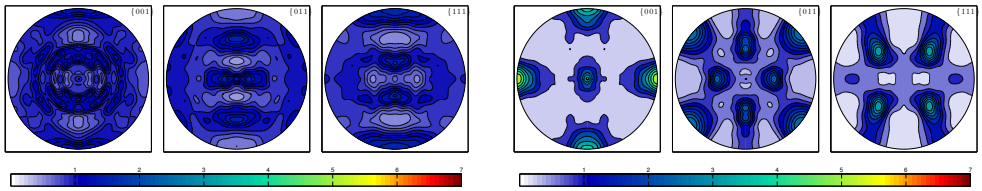

(C) 400 orientations

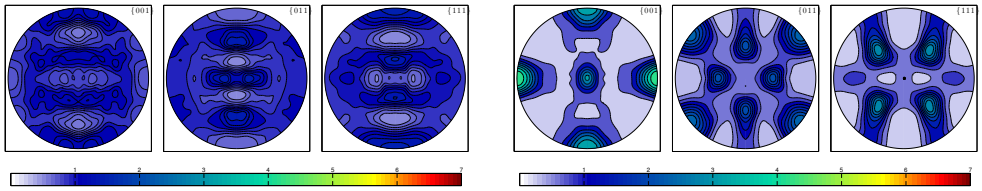

(D) 825 orientations

FIGURE 6. Initial pole figures for 1) OFHC copper and 2) 6016 Aluminum

From this figure, it is evident that an ODF with 825 orientations seems to be of acceptable accuracy for texture representation.

For the hexagonal texture, the representative orientations required were higher than that of cubic metals. The zirconium texture also had very dominant features in the pole figures, making it more difficult to fit.

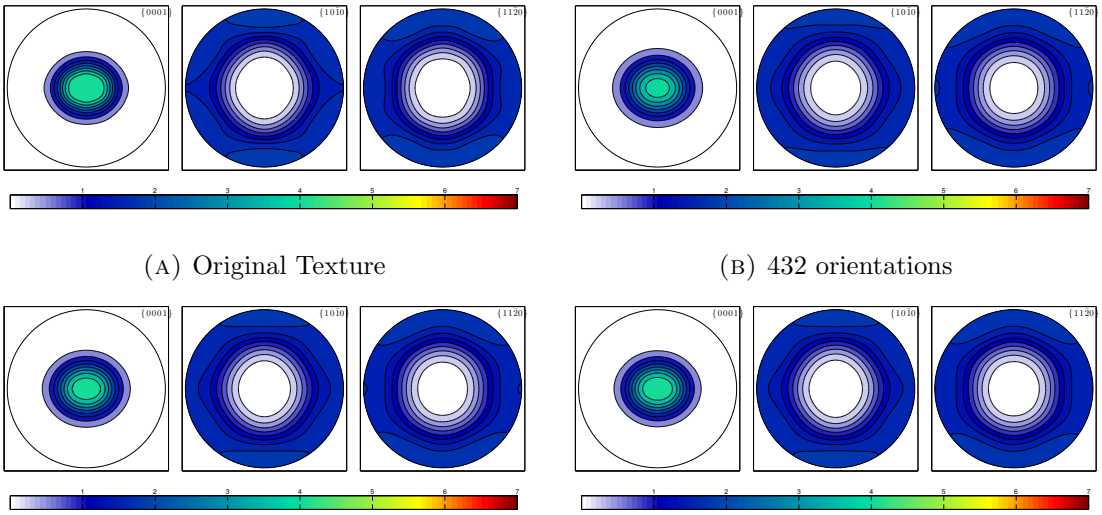

(A) Original Texture

(B) 432 orientations

(C) 1024 orientations

(D) 1600 orientations

FIGURE 7. Initial pole figures for Zr

From the pole figures, the texture is effectively matched even down to 432 orientations. Thus, the minimum data set size should be determined by simulating the stress-strain response and measuring the texture difference post-deformation.

4.2. **Stress-Strain Response.** Since cubic metals deform almost exclusively by slip, fewer deformation paths were considered for cubic metals; simple compression and rolling. Shown in Figure 8, the stress-strain response was virtually indistinguishable from the measured texture.

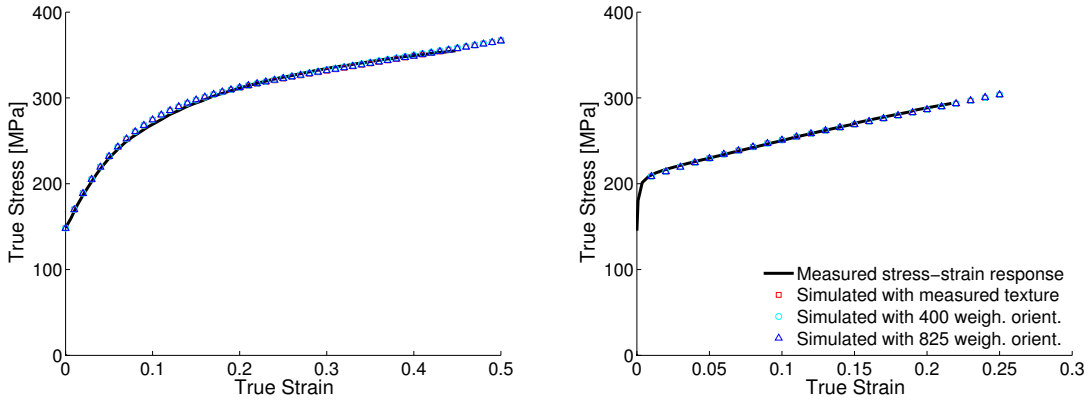

(A) OFHC Cu

(B) Al-6016

FIGURE 8. Stress-strain response for cubic metals under simple compression

The conclusion for cubic metals was that crystalline slip is modeled well with much smaller microstructure data sets. This left the determination of the smallest data set to be based on the difference in texture post-deformation.

Hexagonal metals have a multi-mode deformation mechanism, based on slip and twinning. To verify that the data compaction framework was valid for hexagonal with simple slip, the stress-strain response was simulated at a temperature of 450K, to remove the effect of twinning.

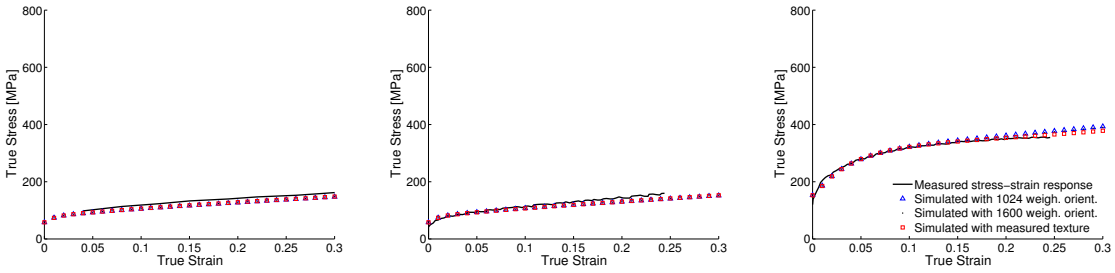

(A) IPT - 450K (B) IPC - 450K (C) TTC - 450K

FIGURE 9. Stress-strain response for Zr without twinning, under different load conditions

From Figure 9, it is clear that smaller data sets still provide an accurate representation of plastic material response. The most stress-strain variance was evident in the TTC curve.

After validating that the framework was symmetry independent, we validated it for the twinning phenomenon. Zr exhibits twinning behavior at lower temperatures, so we used a temperature of 76K in the stress-strain simulation.

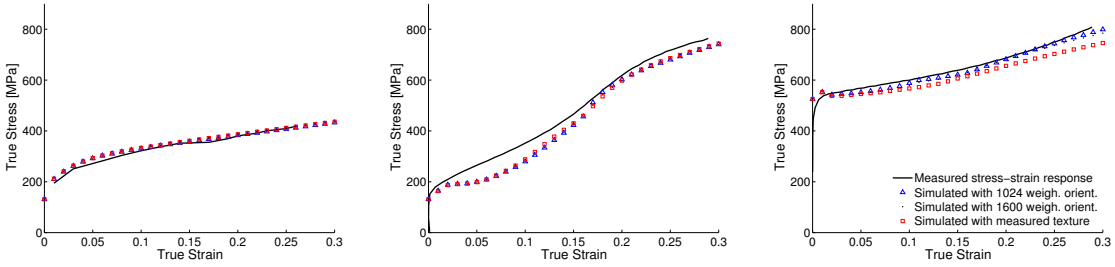

(A) IPT - 76K (B) IPC - 76K (C) TTC - 76K

FIGURE 10. Stress-strain response for Zr with twinning, under different load conditions

Again, the most difference in the stress-strain response was present in the TTC curve, however, the maximum difference between the two curves was 4%. Twinning appears to require the most crystalline orientations, however, if an error of 5% or less is acceptable, then much smaller data sets can be achieved.

4.3. **Post-deformation Texture Difference.** The texture difference post-deformation is important because the crystal microstructure determines the material properties which evolve through forming processes. From the following figures, the texture difference saturated in value after a

certain number of crystals was attained in the ODF. This was helpful in determining the number of crystals used in the representative ODF.

The cubic metals were very dependent on the material used. The OFHC copper was more of a random texture, so it was more easily represented, whereas the 6016 aluminum was strongly anisotropic, which was harder to model.

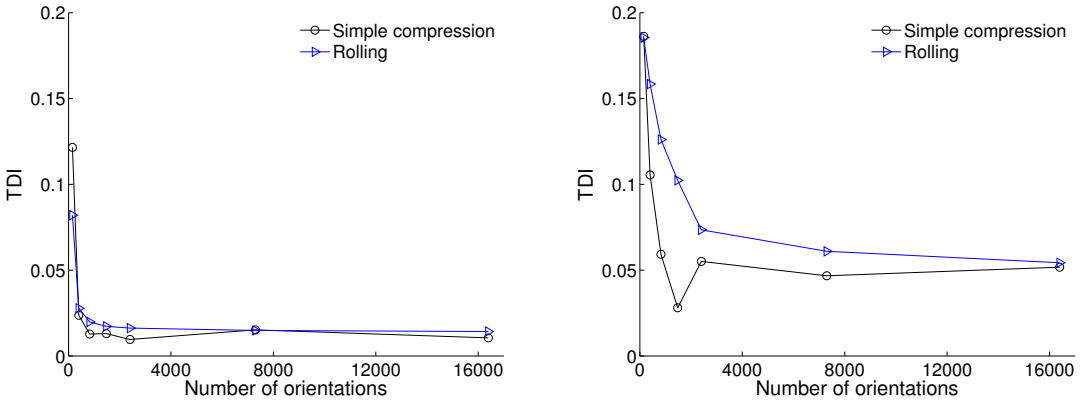

(A) OFHC Cu (B) Al-6016

FIGURE 11. TDI for cubic metals, post-deformation

From Figure 11, the copper TDI saturates quickly, but the aluminum stabilizes at about 2400 orientations, however, the difference is acceptable at 825 orientations.

The hexagonal metals appear to gain accuracy rapidly up to 1600 orientations, then start to asymptotically approach a saturated value with larger data sets.

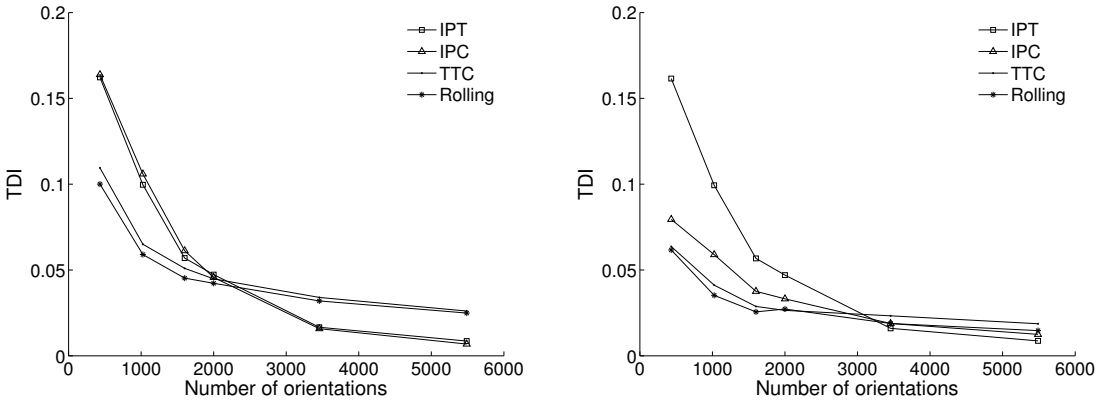

(A) 450K (B) 76K

FIGURE 12. TDI for Zr with and without twinning, post-deformation

From Figure 12, an effective representative ODF size for hexagonal metals appears to be 1600 orientations.

5. Conclusions

This project accomplished two main goals; the development of an effective fitting algorithm to generate compacted data sets and validation of the framework for data compaction on metals with different material symmetries deforming under slip and twinning. The development of a fitting algorithm by reformulating the problem as a constrained linear optimization and solving with the interior point method has increased the computational speed of fitting a texture by approximately 500 times over the previous algorithm.

The minimum data set was determined to be 825 orientations for both copper and aluminum. The texture differences in copper for this ODF size after deformation by simple compression and rolling are both under 2%. For aluminum, the values are higher (5.9% and 12.6%, for simple compression and rolling respectively). The stress-strain response in both aluminum and copper for compacted data sets was nearly indistinguishable from the objective stress-strain curve.

Generating representative textures for hexagonal metals required more investigation of the discretization of the Euler space to fit more Fourier coefficients. Changing this discretization increased the compactness by a factor of greater than 16. Hexagonal in general was more difficult to represent accurately, however, a minimum of 1600 orientations was validated for zirconium (Zr) with and without twinning. The minimum ODF size was determined to be 1600 because post-deformation texture difference approaches the saturated texture difference value with larger data sets. The texture differences after deformation are reasonable - less than 6% for all modes of deformation.

The significance of this work cannot be underestimated. This compaction method can reduce millions of material microstructure data points or more to 825 orientations for cubic metals and 1600 orientations for hexagonal metals, increasing computational speed potentially by several orders of magnitude. This will contribute to the computational feasibility of microstructure-sensitive forming simulations, which are necessary for microstructure informed design. This data compaction framework will enable microstructure informed design, which will contribute to a genesis in new material development.

6. Acknowledgements

I would like to thank my mentor, Prof. Marko Knezevic, for his guidance and input while I worked on this project. His insight was invaluable as I worked through conceptual and practical challenges. Also, he was always available to ask questions and work through problems, which was much appreciated. I would like to thank the Mechanical Engineering Department of the University of New Hampshire, which has supported me in all my endeavors through the duration of my undergraduate career. Thanks to the Hamel Center for Undergraduate Research for providing support for this research through a SURF grant. Lastly, I would like to thank my family for their tireless support of my education and career interests; it has been a blessing.

7. References

1. Adams, B. L., Surya Kalidindi, and David T. Fullwood. *Microstructure-sensitive Design for Performance Optimization.* Waltham, MA: Butterworth-Heinemann, 2013. Print.

2. Fast, Tony, Marko Knezevic, and Surya R. Kalidindi. "Application of Microstructure Sensitive Design to Structural Components Produced from Hexagonal Polycrystalline Metals." *Computational Materials Science* 43 (2008): 374-83. *ScienceDirect.* Web.

3. Shaffer, Joshua B., Marko Knezevic, and Surya R. Kalidindi. "Building Texture Evolution Networks for Deformation Processing of Polycrystalline FCC Metals Using Spectral Approaches: Applications to Process Design for Targeted Performance." *International Journal of Plasticity* 26 (2010): 1183-194. *ScienceDirect.* Web.

4. Fromm, Bradley S., Brent L. Adams, Sadegh Ahmadi, and Marko Knezevic. "Grain Size and Orientation Distributions: Application to Yielding of A-titanium." *Acta Materialia* 57 (2009): 2339-348. *ScienceDirect.* Web.

5. Knezevic, Marko, Hamad F. Al-Harbi, and Surya R. Kalidindi. "Crystal Plasticity Simulations Using Discrete Fourier Transforms." *Acta Materialia* 57 (2009): 1777-784. *ScienceDirect.* Web.

6. Wiess, Rick. "About the Materials Genome Initiative." *The White House.* Executive Office of the President of the United States, n.d. Web. 27 Oct. 2013.

7. Wu, X., G. Proust, M. Knezevic, and S. R. Kalidindi. "Elastic-plastic Property Closures for Hexagonal Close-packed Polycrystalline Metals Using First-order Bounding Theories." *Acta Materialia* 55 (2007): 2729-737. *ScienceDirect.* Web.

8. Kalidindi, Surya R., Marko Knezevic, Stephen Niezgoda, and Joshua Shaffer. "Representation of the Orientation Distribution Function and Computation of First-order Elastic Properties Closures Using Discrete Fourier Transforms." *Acta Materialia* 57 (2009): 3916-923. *ScienceDirect.* Web.

9. Knezevic, Marko. "Microstructure Based Models for Predicting Deformation Behavior of Polycrystalline Metals." The University of New Hampshire, Durham. Dec. 2012. Lecture.

10. Bunge, H.J. *Texture Analysis in Materials Science: Mathematical Methods.* London: Butterworths, 1982. Print.

11. Tomé, C.N., and R.A. Lebensohn. *Manual for Code - VISCO-PLASTIC SELF-CONSISTENT (VPSC) Version 7c.* Manual. N.p.: Los Alamos National Laboratory, 2009. Print.

12. Randle, V., and Olaf Engler. *Introduction to Texture Analysis: Macrotexture, Microtexture and Orientation Mapping.* Amsterdam, The Netherlands: Gordon & Breach, 2000. Print.